

# Twinning is not shearing: Case of the extension twins in magnesium

Cyril Cayron

Laboratory of ThermoMechanical Metallurgy (LMTM), PX Group Chair, Ecole Polytechnique Fédérale de Lausanne (EPFL), Rue de la Maladière 71b, 2000 Neuchâtel, Switzerland

## Abstract

A crystallographic model is proposed for the extension twins in magnesium. It is based on a hard-sphere assumption previously used for martensitic transformations, and it reverses the approach of the classical theory of mechanical twinning. First, the atomic displacements are established, and then the lattice distortion is calculated and analytically expressed as a continuous angular-distortive matrix that takes the form of usual shear only when the distortion is complete. The calculations prove that a volume change of 3% occurs during the intermediate states and that the twinning plane, even if globally invariant (untilted and restored), is not fully invariant. Consequently, extension twinning is not a shear mechanism. An energetical criterion based on the value of the intermediate distortion matrix at the maximum volume change is proposed to replace the usual Schmidt law. It allows predicting the formation of extension twins for tensile conditions and crystal orientations associated with negative Schmid factors.

**Keywords :** Extension twins, magnesium, Schmid factor, angular-distortive matrix, hard-sphere

## 1. Introduction

Mechanical twinning is usually considered as a shear transformation [1]-[6]. For example Bevis and Crocker [3] adopted the definition “*twinning shear is any shear which restores a lattice in a new orientation*” and used it to build a generalized theory that predicts the possible twinning matrices. The realistic ones were chosen among those with the minimum shearing magnitude. The belief that mechanical twinning is a shear deformation relies on the observations of planar interfaces between the parent and its twins. As explained by Christian and Mahajan [4]: “*Since a parent crystal and its twin remain in contact at the interface plane during the formation of the twin, the relation between the structures must be such that this plane is invariant in any deformation carrying one lattice into the other*”. Consequently, the classical theory of twinning makes a large use of shear planes and shear directions or of their conjugates (see ref. [4] for example). Concerning more particularly the hexagonal close-packed (hcp) metals, fifteen deformation twinning modes could be established in titanium by Crocker and Bevis [5], and a more recent theoretical study also based on lattice

correspondence resulting from shear deformation has been proposed by Niewczas [6] to analyze the correspondence of the dominant slip modes in the parent and its twins.

Let us now consider more in details twinning in magnesium. Magnesium, thanks to its lightness, is used in some automotive parts and considered as a good candidate for many other applications, but it suffers from a poor ductility, because, as other hcp metals, its number of slip systems is low. Twinning comes as an additional important deformation mechanism that improves the elongation, but in a very anisotropic way. A better understanding of deformation twinning could thus help to improve the mechanical properties and enlarge the use of magnesium alloys in industry. The main twinning modes observed in magnesium are the “extension” twins on the  $\{10\bar{1}2\}$  planes that usually form when the **c**-axis is close to the tensile axis, the “compression” twins on the  $\{10\bar{1}1\}$  planes that usually form when the **c**-axis crystal is close to the compression axis, and the so-called  $\{10\bar{1}1\}$ - $\{10\bar{1}2\}$  “double”-twins that are supposed to the result from a double-step compression-extension mechanism. The twinning modes were historically determined from the trace of the habit planes in deformed single crystals [7], and they are now currently and automatically identified in single crystal or polycrystalline magnesium by Electron Back Scatter Diffraction (EBSD) by measuring the specific misorientations between a parent grain and the twins it contains (see ref. [8] for example). The twin boundaries of the three twinning modes are all characterized by a rotation around the **a**-axis and differ only by their rotation angle:  $86^\circ$  for the  $\{10\bar{1}2\}$  extension twins,  $56^\circ$  for the  $\{10\bar{1}1\}$  contraction twins, and  $38^\circ$  for the  $\{10\bar{1}1\}$ - $\{10\bar{1}2\}$  “double-twins”. Many questions concerning the twinning mechanisms remain open. The  $\{10\bar{1}2\}$  extension twins and the  $\{10\bar{1}1\}$  compression twins were on the list of the fifteen twin modes predicted by Crocker and Bevis [5], but not the “double-twins”, and many of the predicted modes could not be observed. More surprisingly, many experimental studies report that twins can form despite low or even negative Schmid factors, which was called “anomalous twinning” or “non-Schmid behavior”. Anomalous twinning was reported mainly for the double-twins and compression twins [7][9][10][11], and more recently for the extension twins [12]-[14].

Another unsolved question is the atomic displacements during twinning. In the classical theory, the atoms at the lattice nodes are assumed to follow the lattice shear displacements, and the other atoms should follow other trajectories called “shuffles”. Even if it is agreed that both shear and shuffles are concomitant, the classical theory first establishes the lattice shear, and only then estimates the shuffles without rigorous justification. Very recently, some researchers tried to develop models for extension twinning in which the shear and shuffle displacements really occur simultaneously. Yu et al. [15] proposed a nice two-step rotation-shear model and gave precise atomic trajectories, and Pond et al. [16] proposed a method of shear/shuffle factorization by assuming that deformation twins grow by the motion of disconnections along the interfaces. These models are very interesting but remain stuck on the hypothesis that twinning is a shear mechanism. In addition, these models do not check whether or not the atoms could move without “colliding”. Magnesium is a hcp metal with a ratio  $\frac{c}{a} = 1.623$  very close to the theoretical ratio  $\frac{c}{a} = \frac{4}{\sqrt{6}} \approx 1.633$  expected from a hard-sphere model, which means the atoms should be considered as hard-spheres, and any equation of atomic path should check that the atoms do not interpenetrate.

Another point is puzzling. Recently, Liu et al. [17][18] reported in-situ TEM observations of extension twins in a submicron-sized single crystal Mg pillar induced by compression along the  $[1\bar{1}0]$  axis.

Surprisingly, the orientation relationship between the parent crystal and its twin is a rotation of 90° around the **a**-axis, in place of the expected 86° rotation. In addition, the parent/twin interface is made of basal/prismatic terrace-like interfaces instead of a straight boundary along a {10̄12} plane. They also observed that the interface can propagate reversibly without obvious shear. These results made the authors assume that the extension twins they observed were not produced by a simple shear but by a “*newly discovered deformation mode*”. This mode implies a direct conversion between the basal and prismatic planes of the parent crystal and its twin resulting in a tetragonal compression of the lattice. The authors proposed a model based on a type of atomic rearrangements that they called “unit cell reconstruction”, which seems in contradiction with the displacive character of mechanical twinning. This probably explains why the model was received with reservations [16][19]. For example, Ostapovets *et al.* [19] gave another explanation to the experimental results. They showed that the tetragonal deformation matrix is the stretch component that appears in the polar decomposition of the usual simple shear matrix, and they proposed that the 90° twins are “produced by an average of two conjugate simple shears”. However, Ostapovets *et al.* could not give any further details on the physical nature of the average, and they did not explain why the traces of the two compensating shearing planes could not be observed by Liu *et al.* in the submicron-sized Mg pillars.

The aim of the present paper is to propose, in the case of the extension twins in magnesium, an alternative approach to the classical model of deformation twinning. This follows our recent developments in the crystallography of martensitic transformation in steels [20], and more generally between the fcc, bcc and hcp phases [21]. The case of mechanical twinning in fcc crystals was also treated in ref.[21]. The model consists in considering that the atoms are hard spheres of constant size and that the lattice distortion must respect the size of the atoms in order to avoid their interpenetration. It was used to prove that martensitic transformations in compact alloys are not shear mechanisms or combination of them, contrarily to the usual point of view. The same approach is used here to prove that the habit plane of the {10̄12} extension twins is not fully invariant, and that a small volume change occurs during the lattice distortion; which means that extension twinning in magnesium is not a shear mechanism, neither. The atomic displacements will be calculated in a continuous way. The results obtained by Liu *et al.* will be discussed. An energetic criterion replacing the Schmid factor will be proposed. Some of the experimental results reported in literature on “anomalous” twinning will be explained with this new criterion. The paper concerns only the {10̄12} extension twins; another paper about the {10̄11} and {10̄11}-{10̄12} compression twins is in preparation.

## 2. Notations and calculation rules

The three-index notation in the hexagonal system is preferentially chosen for the calculations. The planes will be sometimes written in four-index notation, but mainly to refer to literature. The vectors are noted by bold lowercase letters and the matrices by bold capital letters. The Mg atoms are considered as hard spheres of constant size. The ratio of lattice parameters taken in the calculations is the ideal hcp ratio:

$$c/a = 4/\sqrt{6} \quad (1)$$

We call  $\mathbf{B}_{hex} = (\mathbf{a}, \mathbf{b}, \mathbf{c})$  the usual hexagonal basis, and  $\mathbf{B}_{ortho} = (\mathbf{x}, \mathbf{y}, \mathbf{z})$  the orthonormal basis represented in Fig. 1 and linked to  $\mathbf{B}_{hex}$  by the coordinate transformation matrix  $\mathbf{H}_{hex}$ :

$$\mathbf{H}_{hex} = [\mathbf{B}_{ortho} \rightarrow \mathbf{B}_{hex}] = \begin{pmatrix} 1 & -1/2 & 0 \\ 0 & \sqrt{3}/2 & 0 \\ 0 & 0 & c/a \end{pmatrix} \quad (2)$$

In order to follow the displacements of the Mg atoms during extension twinning, some labels are given to the atomic positions, as illustrated in Fig. 1. We note O, the “zero” position that will be let invariant by the distortion. We call X, Y and Z the atomic positions defined by the vectors  $\mathbf{O}\mathbf{X} = \mathbf{a} = [100]_{hex}$ ,  $\mathbf{O}\mathbf{Y} = \mathbf{a} + 2\mathbf{b} = [120]_{hex}$  and  $\mathbf{O}\mathbf{Z} = \mathbf{c} = [001]_{hex}$ . It can be checked with the matrix  $\mathbf{H}_{hex}$  that  $\mathbf{O}\mathbf{X} = [100]_{ortho}$ ,  $\mathbf{O}\mathbf{Y} = [0 \sqrt{3} 0]_{ortho}$  and  $\mathbf{O}\mathbf{Z} = [0 0 c/a]_{ortho}$ . The nodes O, X, Y, Z define a non-primitive cell that will be noted XYZ. Other vectors are noted  $\mathbf{O}\mathbf{S} = \mathbf{O}\mathbf{X} + \mathbf{O}\mathbf{Y} = [220]_{hex}$ ,  $\mathbf{O}\mathbf{T} = \mathbf{O}\mathbf{X} + \mathbf{O}\mathbf{Z} = [101]_{hex}$ ,  $\mathbf{O}\mathbf{U} = \mathbf{O}\mathbf{S} + \mathbf{O}\mathbf{Z} = [221]_{hex}$ ,  $\mathbf{O}\mathbf{V} = \mathbf{O}\mathbf{Y} + \mathbf{O}\mathbf{Z} = [121]_{hex}$ . The atoms in the center of the face (O, X, Y, S) is noted are noted M, and the atom close to the face (O, X, Z, T) is noted N; their position vectors are  $\mathbf{O}\mathbf{M} = [110]_{hex}$  and  $\mathbf{O}\mathbf{N} = [2/3, 1/3, 1/2]_{hex}$ . At the same z-level as N, there are the positions P and Q given by  $\mathbf{O}\mathbf{P} = [5/3, 4/3, 1/2]_{hex}$  and  $\mathbf{O}\mathbf{Q} = [2/3, 4/3, 1/2]_{hex}$ . Additional positions without atom will be used in the calculations; they are I middle of OX, J middle of OY, and K middle of OZ (Fig. 1d). The bases in which the vectors and matrices are expressed are specified in the text or as indices in the equations.

To describe the crystallography of extension twinning  $p \rightarrow t$  from a parent crystal  $p$  to its twin  $t$ , three important matrices will be used: the distortion matrix, the coordinate transformation matrix, and the correspondence matrix. Let us briefly explain them.

The distortion matrix  $\mathbf{D}$  gives the image  $\mathbf{x}'$  of a vector  $\mathbf{x}$  by a displacive transformation:  $\mathbf{x}' = \mathbf{D} \cdot \mathbf{x}$ . The displacement field is given by  $\mathbf{x}' - \mathbf{x} = (\mathbf{D} - \mathbf{I}) \cdot \mathbf{x}$  where  $\mathbf{I}$  is the 3x3 identity matrix. The deformation matrix is given by its gradient, i.e. the matrix  $\mathbf{D} - \mathbf{I}$ . The letter  $\mathbf{F}$  is often used in place of  $\mathbf{D}$  in the finite strain theory. The letter  $\mathbf{U}$  will be preferred to  $\mathbf{D}$  to specify that the distortion matrix is symmetric. The distortion matrix can be calculated as follows. The vectors of the initial parent basis are transformed by the distortion into new vectors:  $\mathbf{a}_p \rightarrow \mathbf{a}'_p$ ,  $\mathbf{b}_p \rightarrow \mathbf{b}'_p$  and  $\mathbf{c}_p \rightarrow \mathbf{c}'_p$ . The distortion matrix  $\mathbf{D}^{p \rightarrow t}$  is the matrix formed by the images  $\mathbf{a}'_p$ ,  $\mathbf{b}'_p$  and  $\mathbf{c}'_p$  expressed in the initial basis, i.e.  $\mathbf{D}^{p \rightarrow t} = [\mathbf{B}_{hex}^p \rightarrow \mathbf{B}_{hex}^{p'}]$  with  $\mathbf{B}_{hex}^p = (\mathbf{a}_p, \mathbf{b}_p, \mathbf{c}_p)$  and  $\mathbf{B}_{hex}^{p'} = (\mathbf{a}'_p, \mathbf{b}'_p, \mathbf{c}'_p)$ . This matrix expressed in the basis  $\mathbf{B}_{hex}^p$  is simply  $\mathbf{D}_{hex}^{p \rightarrow t} = \mathbf{B}_{hex}^{p'}$  formed by writing the coordinates of  $\mathbf{a}'_p$ ,  $\mathbf{b}'_p$  and  $\mathbf{c}'_p$  in column. The crystallographic studies on displacive phase transformations and mechanical twinning often consist in finding the distortion matrix with the lowest values in order to minimize the atomic displacements. If the matrix  $\mathbf{D}^{p \rightarrow t}$  is found in the basis  $\mathbf{B}_{ortho}$ , and noted  $\mathbf{D}_{ortho}^{p \rightarrow t}$ , a formula of coordinate transformation can be used to express it in the basis  $\mathbf{B}_{hex}$ ; it is:

$$\mathbf{D}_{hex}^{p \rightarrow t} = \mathbf{H}_{hex}^{-1} \mathbf{D}_{ortho}^{p \rightarrow t} \mathbf{H}_{hex} \quad (3)$$

Inversely, if the distortion matrix is found in  $\mathbf{B}_{hex}$  and it can be written in  $\mathbf{B}_{ortho}$  by the formula:

$$\mathbf{D}_{ortho}^{p \rightarrow t} = \mathbf{H}_{hex} \mathbf{D}_{hex}^{p \rightarrow t} \mathbf{H}_{hex}^{-1} \quad (4)$$

The coordinate transformation matrix  $\mathbf{T}^{p \rightarrow t}$  is used to change the coordinates of a fixed vector between the parent and twin bases. It is given by the vectors of the basis of the twin  $\mathbf{B}_{hex}^t = (\mathbf{a}_t, \mathbf{b}_t, \mathbf{c}_t)$  expressed in the parent basis, i.e.  $\mathbf{T}^{p \rightarrow t} = [\mathbf{B}_{hex}^p \rightarrow \mathbf{B}_{hex}^t]$ . This matrix can be calculated

from the orientation relationship between the parent and its daughter twin deduced from experimental observations by optical microscopy and X-ray diffraction on single crystals, or transmission electron microscopy (TEM) or Electron backscatter Diffraction (EBSD) on single or polycrystalline materials. The coordinate transformation matrix for the reverse twinning operation is simply  $\mathbf{T}^{t \rightarrow p} = (\mathbf{T}^{p \rightarrow t})^{-1}$ .

The images  $\mathbf{a}'_p$ ,  $\mathbf{b}'_p$  and  $\mathbf{c}'_p$  can be expressed in the twin basis by using the coordinate transformation matrix. The three vectors written in column form a matrix  $(\mathbf{a}'_p, \mathbf{b}'_p, \mathbf{c}'_p)_{/\mathbf{B}_{hex}^t} = \mathbf{T}^{t \rightarrow p} (\mathbf{a}'_p, \mathbf{b}'_p, \mathbf{c}'_p)_{/\mathbf{B}_{hex}^p} = \mathbf{T}^{t \rightarrow p} \mathbf{B}_{hex}^{t \rightarrow p} = \mathbf{T}^{t \rightarrow p} \mathbf{D}^{p \rightarrow t}$  called the correspondence matrix  $\mathbf{C}^{t \rightarrow p}$ , i.e.

$$\mathbf{C}^{t \rightarrow p} = \mathbf{T}^{t \rightarrow p} \mathbf{D}^{p \rightarrow t} \quad (5)$$

### 3. Stretch component of the complete distortion matrix

As recalled in introduction, we consider that the lattice distortion is a consequence of the atomic displacement; however, in order to help the reading and make a link with the usual view, this section directly calculates the matrix of lattice distortion in the case of a complete transformation, without considering the continuous path that leads to it.

Let consider the case of extension twinning such that the axis  $\mathbf{a}$  remains invariant, the axis  $\mathbf{a}+2\mathbf{b}$  of the parent crystal is transformed into the axis  $\mathbf{c}$  of the twin, and the axis  $\mathbf{c}$  of the parent is transformed into the axis  $\mathbf{a}+2\mathbf{b}$  of the twin:

$$\mathbf{a}'_p = \mathbf{a}_t, \quad \mathbf{a}'_p + 2\mathbf{b}'_p = \mathbf{c}_t, \quad \mathbf{c}'_p = \mathbf{a}_t + 2\mathbf{b}_t \quad (6)$$

which by linear combination gives

$$\mathbf{a}'_p = \mathbf{a}_t, \quad \mathbf{b}'_p = \frac{1}{2}(\mathbf{c}_t - \mathbf{a}_t), \quad \mathbf{c}'_p = \mathbf{a}_t + 2\mathbf{b}_t \quad (7)$$

Thus, the correspondence matrix  $\mathbf{C}^{t \rightarrow p}$  of extension twinning expressed in the basis  $\mathbf{B}_{hex}$  is:

$$\mathbf{C}_{hex}^{t \rightarrow p} = \begin{pmatrix} 1 & -1/2 & 1 \\ 0 & 0 & 2 \\ 0 & 1/2 & 0 \end{pmatrix} \quad (8)$$

If there is no additional rotation, the twin becomes misoriented from its parent by a rotation of 90° around the invariant axis  $\mathbf{a}_p = \mathbf{a}_t$ . The coordinate transformation matrix  $\mathbf{T}_{hex}^{p \rightarrow t}$  is given by the vectors of the twin basis expressed in the parent basis. In the present case, this matrix is similar to the correspondence matrix, excepted that now the metrics appears:

$$\mathbf{T}_{hex}^{p \rightarrow t} = \begin{pmatrix} 1 & -1/2 & \frac{1}{\sqrt{3}}(c/a) \\ 0 & 0 & \frac{2}{\sqrt{3}}(c/a) \\ 0 & \frac{\sqrt{3}}{2}(a/c) & 0 \end{pmatrix} = \begin{pmatrix} 1 & -1/2 & \frac{2\sqrt{2}}{3} \\ 0 & 0 & \frac{4\sqrt{2}}{3} \\ 0 & \frac{3}{4\sqrt{2}} & 0 \end{pmatrix} \quad (9)$$

The distortion matrix  $\mathbf{U}_{hex}^{p \rightarrow t}$  is obtained from the correspondence and coordinate transformation matrices by using equation (5):

$$\mathbf{U}_{hex}^{p \rightarrow t} = \mathbf{T}_{hex}^{p \rightarrow t} \mathbf{C}_{hex}^{t \rightarrow p} = \begin{pmatrix} 1 & -\frac{1}{2} + \frac{\sqrt{2}}{3} & 0 \\ 0 & \frac{2\sqrt{2}}{3} & 0 \\ 0 & 0 & \frac{3}{2\sqrt{2}} \end{pmatrix} \quad (10)$$

This matrix is given in the basis  $\mathbf{B}_{hex}$ . It can be written in the basis  $\mathbf{B}_{ortho}$  by using equation (4):

$$\mathbf{U}_{ortho}^{p \rightarrow t} = \mathbf{H}_{hex} \mathbf{U}_{hex}^{p \rightarrow t} \mathbf{H}_{hex}^{-1} = \begin{pmatrix} 1 & 0 & 0 \\ 0 & \frac{2\sqrt{2}}{3} & 0 \\ 0 & 0 & \frac{3}{2\sqrt{2}} \end{pmatrix} \approx \begin{pmatrix} 1 & 0 & 0 \\ 0 & 0.94 & 0 \\ 0 & 0 & 1.06 \end{pmatrix} \quad (11)$$

This is the matrix already reported in literature [17][19]. This matrix is diagonal; it is a stretch equivalent to the Bain distortion known in martensitic transformations. The diagonal values are  $x'/x$ ,  $y'/y$ ,  $z'/z$ ; they mean that the distortion lets the **x**-axis invariant, shorten the **y**-axis by  $\Delta y/y = -6\%$  and extends the **z**-axis by  $\Delta z/z = +6\%$ . This explains why this type of twins is an extension twin formed during tensile test along the **c**-axis. The ratio of contraction  $y'/y$  is exactly the inverse of the ratio of extension  $z'/z$ . One can now raise the question: how the two ratios evolve *during* the lattice distortion? Do they follow this inverse relation continuously? A direct way to answer the question is go deeper into the understanding of the transformation by considering the atomic displacements.

#### 4. Stretch component of the continuous distortion matrix

The mechanistic reason of the simultaneous  $y'/y$  contraction and  $z'/z$  extension is the coordinated displacement of the M and N atoms. Indeed, these atoms are in contact and keep contact during their movement. The atom M initially in the basal plane  $(O, X, Y, S) = (001)_p$  goes out of the plane such that after twinning this plane is transformed into the prismatic plane  $(O, X, Y, S) = (010)_t$ , and the atom N goes toward the prismatic plane  $(010)_p$ , such after twinning this plane is transformed into the basal plane  $(001)_t$ , as illustrated in Fig. 1 and in Fig. 2a and b. During these displacements, the distance OZ increases and the distance OY decreases. It is assumed that the atoms O and X do not move, and that the atoms M and N keep contact with the atoms O and X and between each other during their displacements. The trajectories of the M and N atoms can then be described by a unique parameter, which is the angle  $\eta$  made by the vector **IM** with the basal plane  $(O, X, Y, S)$  (Fig. 1 and Fig. 2). Let us call  $\Phi$  the angle between the direction **IN** with the basal plane  $(O, X, Y, S)$ , i.e.  $\Phi = \text{ArcCos} \left( \frac{1}{3} \right) \approx 70.5^\circ$ . During extension twinning, the angle  $\eta$  increases from the starting value  $\eta_s = 0$  to the finishing value  $\eta_f = \frac{\pi}{2} - \Phi \approx 19.47^\circ$ . The coordinates of the atoms M and N in the orthonormal basis  $\mathbf{B}_{ortho}$  are

$$\mathbf{OM} = \begin{pmatrix} 1/2 \\ \frac{\sqrt{3}}{2} \cos(\eta) \\ \frac{\sqrt{3}}{2} \sin(\eta) \end{pmatrix} \quad \text{and} \quad \mathbf{ON} = \begin{pmatrix} 1/2 \\ \frac{\sqrt{3}}{2} \cos(\eta + \Phi) \\ \frac{\sqrt{3}}{2} \sin(\eta + \Phi) \end{pmatrix} \quad (12)$$

In the present case, it is supposed that during the transformation  $\mathbf{OY}'$  remains parallel to  $\mathbf{OY}$ . The atom M moves such that it keeps contact with the atoms O, X and Y. Thus, as shown in Fig. 2d, the point J in the middle of OY keeps the same y-coordinate as M during the distortion, i.e.  $OY = 2 OJ = \sqrt{3} \cos(\eta)$ . It is also assumed that  $OZ'$  remains parallel to  $OZ$ . The atom N moves such that it keeps contact with the atoms O, X and Z. Thus, as shown in Fig. 2d, the point K in the middle of OZ keeps the same z-coordinate as N during the distortion, i.e.  $OZ = 2 OK = \sqrt{3} \sin(\eta + \Phi)$ . Let us write the vectors  $\mathbf{OX}$ ,  $\mathbf{OY}$  and  $\mathbf{OZ}$  forming the basis  $\mathbf{B}_{XYZ}$  of the  $XYZ$  cell in the orthonormal basis  $\mathbf{B}_{ortho}$ . The coordinate transformation matrix between the bases  $\mathbf{B}_{ortho}$  and  $\mathbf{B}_{XYZ}$  is

$$[\mathbf{B}_{ortho} \rightarrow \mathbf{B}_{XYZ}(\eta)] = \mathbf{B}_{XYZ}(\eta) = \begin{pmatrix} 1 & 0 & 0 \\ 0 & \sqrt{3} \cos(\eta) & 0 \\ 0 & 0 & \sqrt{3} \sin(\eta + \Phi) \end{pmatrix} \quad (13)$$

The continuous distortion matrix at each step  $\eta$  of the transformation is given in the basis  $\mathbf{B}_{ortho}$  by the matrix  $\mathbf{U}_{ortho}^{p \rightarrow t}(\eta) = \mathbf{B}_{XYZ}(\eta) \cdot \mathbf{B}_{XYZ}^{-1}(\eta_s)$  (see equation 1 of ref.[1]). The calculation leads to

$$\mathbf{U}_{ortho}^{p \rightarrow t}(\eta) = \begin{pmatrix} 1 & 0 & 0 \\ 0 & \cos(\eta) & 0 \\ 0 & 0 & \frac{3}{2\sqrt{2}} \sin(\eta + \Phi) \end{pmatrix} \quad (14)$$

Let us use the variable  $\kappa = \sin(\eta)$ . The starting value is  $\kappa_s = 0$  and the finish value is  $\kappa_f = 1/3$ . The distortion matrix is a function of  $\kappa$ :

$$\mathbf{U}_{ortho}^{p \rightarrow t}(\kappa) = \begin{pmatrix} 1 & 0 & 0 \\ 0 & \sqrt{1 - \kappa^2} & 0 \\ 0 & 0 & \frac{\kappa}{2\sqrt{2}} + \sqrt{1 - \kappa^2} \end{pmatrix} \quad (15)$$

The matrix of complete transformation is given for  $\kappa_f = 1/3$ ; it can be checked it is the matrix already given in equation (11). It proves that the ratio of contraction  $y'/y$  is the inverse of the ratio of extension  $z'/z$  only in the final state, but not during the distortion.

The distortion matrix can be written in the hexagonal basis  $\mathbf{B}_{hex}$  by using equation (3):

$$\mathbf{U}_{hex}^{p \rightarrow t}(\kappa) = \begin{pmatrix} 1 & \frac{-1 + \sqrt{1 - \kappa^2}}{2} & 0 \\ 0 & \sqrt{1 - \kappa^2} & 0 \\ 0 & 0 & \frac{\kappa}{2\sqrt{2}} + \sqrt{1 - \kappa^2} \end{pmatrix} \quad (16)$$

The ratio of volume change  $\mathcal{V}'/\mathcal{V}$  is directly given by the determinant of the distortion matrix:

$$\frac{\mathcal{V}'}{\mathcal{V}}(\kappa) = \det(\mathbf{U}_{hex}^{p \rightarrow t}) = \det(\mathbf{U}_{ortho}^{p \rightarrow t}) = 1 - \kappa^2 + \frac{\sqrt{2}}{4} \kappa \sqrt{1 - \kappa^2} \quad (17)$$

The curve  $\mathcal{V}'/\mathcal{V}$  is presented in Fig. 3. The maximum of volume change, close to 1.0303 is obtained for the intermediate value  $\kappa_i \approx 0.1691$  ( $\eta_i \approx 9.73^\circ$ ). It proves that, although it returns to its initial value when the distortion is complete, the volume is not constant during the twinning process. Thus, the present approach proves that extension twinning cannot be obtained at constant volume, which means that simple shear matrices are not appropriate to describe the continuous paths of the atoms. A similar conclusion was drawn on fcc-fcc mechanical twinning in a previous study (sections 3 and 7.5 of ref.[1]).

The matrix  $\mathbf{U}_{hex}^{p \rightarrow t}(\kappa)$ , with  $\kappa = \text{Sin}(\eta)$ , gives the stretch (Bain) matrix during the process of extension twinning. The atoms at the first corners of the XYZ cell (i.e. O, X, Y, Z) follow a trajectory whose equation in the basis  $\mathbf{B}_{ortho}$  is directly given by this matrix, with  $\kappa$  continuously varying from  $\kappa_s = 0$  to  $\kappa_f = 1/3$ . The atoms M, N, Q inside the XYZ cell do not follow the same trajectory; they “shuffle”. The trajectory equation of M and N is deduced from equation (12). Actually, the initial position vectors in the basis  $\mathbf{B}_{ortho}$ , which are  $\mathbf{OM} = \left[ \frac{1}{2}, \frac{\sqrt{3}}{2}, 0 \right]$ ,  $\mathbf{ON} = \left[ \frac{1}{2}, \frac{\sqrt{3}}{6}, \frac{\sqrt{6}}{3} \right]$ ,  $\mathbf{OQ} = \left[ 0, \frac{2\sqrt{3}}{3}, \frac{\sqrt{6}}{3} \right]$ , are all rotated by the same “shuffle rotation” that is simply

$$\mathbf{R}_{shuffle}(\eta) = \begin{pmatrix} 1 & 0 & 0 \\ 0 & \text{Cos}(\eta) & -\text{Sin}(\eta) \\ 0 & \text{Sin}(\eta) & \text{Cos}(\eta) \end{pmatrix} \quad (18)$$

Consequently, in the XYZ cell, the corner atoms O, X, Y, Z, S, T, U, V (each of them count for 1/8 in the cell) follow the distortion (15), and the atom M (counts for 1/2), N (counts for 1), Q (counts for 1/2) follow the shuffling (18). This means that twinning is obtained with 1/3 of distortion and 2/3 of shuffle.

Some movies displaying the atom displacements in a magnesium crystal during the twinning transformation were computed with VPython. The first movie (Supplementary Material 1) shows the transformation of a Bravais unit cell, and the second movie (Supplementary Material 2) shows the transformation of a 4x4x4 XYZ supercell. Three snapshots, taken from these two movies at initial, intermediate and final states, are extracted and given in Fig. 4 and Fig. 5.

## 5. Additional rotation and full expression of the distortion matrix

The distortion matrix (15) is diagonal with values not equal to 1, and thus does not let invariant any direction or plane. It leads to an orientation relationship defined by a  $(90^\circ, \mathbf{a})$  rotation between the parent crystal and its twin, which was observed only in submicron-sized Mg single-crystal [17]. In bulk magnesium, it is known that extension twins let “invariant” the  $\{10\bar{1}2\}$  planes, which implies that the orientation relationship is  $(86^\circ, \mathbf{a})$  and not  $(90^\circ, \mathbf{a})$ . Therefore, in order to make this plane untilted, a rotation should be added to the matrix (15), in same way that a rotation is added to the Bain tensor in fcc-bcc transformations in steels (see for example ref. [22]). As the direction  $\mathbf{OX} = \mathbf{a}$  is already invariant, the  $(0\bar{1}12)$  plane can be maintained untilted by compensating the rotation of the direction  $\mathbf{OV} = [121]_{hex} = [0 \sqrt{3}c]_{ortho} \parallel [0 3 2\sqrt{2}]_{ortho}$ . Let us call  $\xi$  the angle  $(\mathbf{OV}, \mathbf{OV}')$

illustrated in Fig. 6a. This angle is calculated by  $(\mathbf{OV}_{ortho}, \mathbf{U}_{ortho}^{p \rightarrow t} \mathbf{OV}_{ortho})$  with the matrix (15). The calculations show that its cosine  $C_\xi$  is a function of  $\kappa$ :

$$C_\xi(\kappa) = \frac{2\sqrt{2}\kappa + 17\sqrt{1-\kappa^2}}{\sqrt{17}\sqrt{17 - 16\kappa^2 + 4\kappa\sqrt{2 - 2\kappa^2}}} \quad (19)$$

The angle  $\xi$  varies from 0 to  $3.5^\circ$  during the diagonal distortion. The rotation matrix that compensates the angle  $\xi$  is given in the basis  $\mathbf{B}_{ortho}$  by

$$\mathbf{R}(\kappa) = \begin{pmatrix} 1 & 0 & 0 \\ 0 & C_\xi(\kappa) & \sqrt{1 - C_\xi(\kappa)^2} \\ 0 & -\sqrt{1 - C_\xi(\kappa)^2} & C_\xi(\kappa) \end{pmatrix} \quad (20)$$

We point out here that only the rotation of the direction  $\mathbf{OV}$  can be cancelled, but not its length change. Indeed, the distance  $\|\mathbf{OV}(\kappa)\| = \|\mathbf{U}_{ortho}^{p \rightarrow t}(\kappa) \cdot \mathbf{OV}\|$  calculated from the matrix (15) is not constant. The ratio of length  $OV'$  by its initial value  $OV$  is

$$\frac{OV'}{OV}(\kappa) = \frac{\sqrt{17 - 16\kappa^2 + 4\kappa\sqrt{2 - 2\kappa^2}}}{\sqrt{17}} \quad (21)$$

The graph is given in Fig. 6b. It proves that, although the length  $OV$  returns to its initial value when the distortion is complete, the distance is not constant during the twinning process. Consequently, although the plane  $(0\bar{1}12)$  remains untilted and is eventually restored, this plane is *not* fully invariant during the process. Strictly speaking, one should say that the twinning plane  $(0\bar{1}12)$  is globally invariant (untilted and restored). The volume change and the modification of some distances in the twinning plane during the lattice distortion prove that extension twinning is not a shear mechanism.

The distortion matrix that lets invariant the  $(0\bar{1}12)$  plane is  $\mathbf{D}_{ortho}^{p \rightarrow t}(\kappa) = \mathbf{R}(\kappa) \mathbf{U}_{ortho}^{p \rightarrow t}(\kappa)$ . The calculations show that

$$\mathbf{D}_{ortho}^{p \rightarrow t}(\kappa) = \begin{pmatrix} 1 & 0 & 0 \\ 0 & \frac{17 - 17\kappa^2 + 2\kappa\sqrt{2 - 2\kappa^2}}{\sqrt{17} d(\kappa)} & \frac{3\kappa(\kappa + 2\sqrt{2 - 2\kappa^2})}{2\sqrt{34} d(\kappa)} \\ 0 & -\frac{3\kappa\sqrt{1 - \kappa^2}}{\sqrt{17} d(\kappa)} & \frac{68 - 64\kappa^2 + 25\kappa\sqrt{2 - 2\kappa^2}}{4\sqrt{17} d(\kappa)} \end{pmatrix} \quad (22)$$

with  $d(\kappa) = \sqrt{17 - 16\kappa^2 + 4\kappa\sqrt{2 - 2\kappa^2}}$

The atomic trajectories could be plotted by using those defined at the end of section 4 and applying the additional rotation (20). They can also be explicitly determined. The matrix  $\mathbf{D}_{ortho}^{p \rightarrow t}(\kappa)$  is the full form of the lattice distortion during extension twinning. The displacements of the atoms at the corners of the XYZ cell (i.e. O, X, Y, Z) follow a trajectory whose equation in the basis  $\mathbf{B}_{ortho}$  is

directly given by this matrix, with  $\kappa$  continuously varying from  $\kappa_s = 0$  to  $\kappa_f = 1/3$ . The atoms M, N, Q shuffle in the XYZ cell. Their trajectories are given by the “shuffling rotation” (18) compensated of the angle  $\xi$ , i.e.

$$\mathbf{R}_{shuffle}(\eta) = \begin{pmatrix} 1 & 0 & 0 \\ 0 & \cos(\eta - \xi) & -\sin(\eta - \xi) \\ 0 & \sin(\eta - \xi) & \cos(\eta - \xi) \end{pmatrix} \quad (23)$$

with  $\xi$  function of  $\eta$  by equation (19).

A movie of the transformation of 4x4x4 XYZ cell is reported in Supplementary Material 3. Three snapshots taken at initial, intermediate and final states are extracted and shown in Fig. 7. It can be checked that the (0112) plane is not tilted during the transformation. Its angular distortion due to the change of length OV is hardly perceptible because of its low value (+1.4%).

## 6. Complete forms of the distortion matrix

When the transformation is complete, the distortion matrix takes the value

$$\mathbf{D}_{ortho}^{p \rightarrow t} = \mathbf{D}_{ortho}^{p \rightarrow t}(1/3) = \begin{pmatrix} 1 & 0 & 0 \\ 0 & \frac{16}{17} & \frac{3}{34\sqrt{2}} \\ 0 & -\frac{2\sqrt{2}}{51} & \frac{18}{17} \end{pmatrix} \quad (24)$$

In the hexagonal basis  $\mathbf{B}_{hex}$ , it becomes, by using equation (3),

$$\mathbf{D}_{hex}^{p \rightarrow t} = \begin{pmatrix} 1 & -\frac{1}{34} & \frac{1}{17} \\ 0 & \frac{16}{17} & \frac{2}{17} \\ 0 & -\frac{1}{34} & \frac{18}{17} \end{pmatrix} \quad (25)$$

In the reciprocal space, one must take the inverse of the transpose:

$$(\mathbf{D}_{ortho}^{p \rightarrow t})^* = (\mathbf{D}_{ortho}^{p \rightarrow t})^{-T} = \begin{pmatrix} 1 & 0 & 0 \\ 0 & \frac{18}{17} & \frac{2\sqrt{2}}{51} \\ 0 & -\frac{3}{34\sqrt{2}} & \frac{16}{17} \end{pmatrix} \quad (26)$$

$$(\mathbf{D}_{hex}^{p \rightarrow t})^* = (\mathbf{D}_{hex}^{p \rightarrow t})^{-T} = \begin{pmatrix} 1 & 0 & 0 \\ \frac{1}{34} & \frac{18}{17} & \frac{1}{34} \\ -\frac{1}{17} & -\frac{2}{17} & \frac{16}{17} \end{pmatrix} \quad (27)$$

The distortion matrix in the direct space and hexagonal frame given by equation (25) has only one eigenvalue equal to 1 and an infinity of eigenvectors that are all linear combinations of the two vectors  $\mathbf{OX} = [100]_{hex}$  and  $\mathbf{OV} = [121]_{hex}$ . This means that the distortion matrix (25) is a simple shear

matrix on the plane  $(0\bar{1}2)_{hex}$ . The shear coefficient  $s$  is the tangent of the angle made by the vector  $\mathbf{n}$  normal of the shear plane with its image. It is easily calculated with  $\mathbf{n} = [0, -c, \sqrt{3}]_{ortho}$  and its image by the matrix (24); it is  $s = \frac{1}{6\sqrt{2}} \approx 0.118$ , as expected from the theoretical value of shear [4].

The shear vector  $\mathbf{s}$  is

$$\mathbf{s} = (\mathbf{D}_{ortho}^{p \rightarrow t} - \mathbf{I}) \cdot \frac{\mathbf{n}}{\|\mathbf{n}\|} = \frac{1}{\sqrt{34}} \left[ 0, \frac{1}{2}, \frac{\sqrt{2}}{3} \right]_{ortho} = \frac{1}{2\sqrt{102}} [121]_{hex} \quad (28)$$

The vector  $\mathbf{s}$  makes an angle of  $43.31^\circ$  with the basal plane. It can be checked that the vector  $\mathbf{s}$  belongs to the “shear” plane  $(0\bar{1}2)_{hex}$ . The distortion matrix expressed in the reciprocal space is given by equation (27); it has only one eigenvalue equal to 1 and an infinity of eigenvectors that are all linear combinations of the two vectors  $(10\bar{1})_{hex}$  and  $(\bar{2}10)_{hex}$ . This means that, in addition to the shear plane  $(0\bar{1}2)_{hex}$ , all the planes that contains the shear vector  $\mathbf{s}$  are also invariant, as expected from a shear matrix.

## 7. Discussion

### A unique mechanism for the $90^\circ$ and $86^\circ$ extension twin domains

The classical model of deformation twinning is based on the lattice correspondences resulting from simple shears; the atomic displacements are not really taken into account; they are inferred as “shuffles” only after determining the lattice shear. The present model reverses the order of thinking. The atomic trajectories are calculated in order to restore the crystal structure in a special orientation relationship. The Mg atoms are assumed to be hard spheres of constant size and their displacements are chosen as low as possible. These assumptions constrain the calculations such that only one parameter, a distortion angle  $\eta$ , is sufficient to follow the trajectories of all the atoms during extension twinning. It is only once the atomic displacements are known that the distortion matrix is calculated as an analytical function of the angular parameter  $\eta$ . First, the calculations were performed assuming the final parent/twin orientation is  $(90^\circ, \mathbf{a})$ , as observed by Liu *et al.* in submicron-sized Mg pillars [17][18], and they confirmed that the distortion matrix is diagonal, i.e. corresponds to a stretch deformation. However, contrarily to the interpretation based on unit cell reconstruction, our model is displacive, as expected for a process implying rapid and collective atomic displacements. Then, we showed that the distortion matrix that lets “invariant” the  $(0\bar{1}2)$  plane differs only from the diagonal form by a small “compensating” rotation angle of  $3.5^\circ$ . In other words, the diagonal distortion matrix related to Liu *et al.*’s observations is the symmetric matrix that can be extracted by polar decomposition from the usual twinning matrix, as already shown by Ostapovest *et al.* [19], in a similar way that Bain tensor appears as a component of the lattice distortion in the fcc-bcc martensitic transformation in steels [20]. However, contrarily to Ostapovest *et al.*’s supposition, we don’t believe that the Liu *et al.*’s observations result from an average of two twinning shear on different conjugate  $\{10\bar{1}2\}$  planes. We think possible that the observed  $(90^\circ, \mathbf{a})$  twins and related stretching described in section 3 actually result from a real “natural” mechanism that is free to appear due the small size of the sample. Indeed, the interface strains required for the basal/prism and prism/basal interfaces (-6% along  $\mathbf{a}+2\mathbf{b}$  and +6% along  $\mathbf{c}$ ) are probably more easily accommodated in the “free” submicron-sized Mg pillar than in bulk Mg. In bulk single crystal or polycrystalline Mg, such strains are too high and need to be reduced, at least

along a  $\{10\bar{1}2\}$  habit plane, by a slight crystal rotation (by  $3.5^\circ$ ). The distortion mechanism in the submicron pillars and in bulk Mg are probably similar. To our point of view, there is a strong analogy between the extension twin domains in magnesium and the orientation domains in ferroelectrics. Let us explain. If, for sake of simplicity, we represent the cubic  $\rightarrow$  tetragonal transition in a ferroelectric crystal by a square  $\rightarrow$  rectangle distortion along the  $x$  and  $y$ -axes four domains misoriented by  $90^\circ$  and  $180^\circ$  rotations should be formed, as illustrated in Fig. 8a. However, experience shows that the domains are actually oriented such that they share one of their two diagonals. There are thus actually height domains, and among them, the  $90^\circ$  misorientation angle is lost and replaced by  $90^\circ-2\delta$ , with  $\delta = \text{Arctan}(a/c)$ , and  $a$  and  $c$  the lattice parameters of the tetragonal phase, as shown in Fig. 8b. The angle  $\delta$  compensates the rotation of the diagonal induced by the tetragonal distortion; it is called obliquity [23][24]. For example, in barium titanate, the tetragonality is close to 1% and  $\delta$  is close to  $0.6^\circ$  [23]. The fact that the diagonal is maintained invariant is explained by strain minimization and compatibility conditions [25][26]. There is a crystallographic equivalence between a) the  $86^\circ = 90^\circ-\xi$  rotation between a  $\{0\bar{1}12\}$  twin and its parent in Mg, and b) the  $90^\circ-2\delta$  rotation between two ferroelectric domains. Following the vocabulary used for ferroelectrics, we would say that the tetragonal distortion observed by Liu *et al.* in the submicron-sized pillars is a “spontaneous” mechanism, and that the angle  $\xi$  required to form the  $\{10\bar{1}2\}$  twins in bulk Mg is an obliquity angle. It may be wondered if the “spontaneous” (or “natural”) distortion is always the one associated with a symmetric distortion matrix, for any twinning or structural phase transformation. This could make sense with symmetry arguments; the daughter phase would share the largest number of symmetry elements and the number of variants would be minimum (the number of variants is the order of the point group of the parent phase divided by the number of common symmetries [27]). However, it is far to be so clear. In the case of fcc-bcc martensitic transformation, our last studies showed that the Bain distortion implies atomic displacements that are larger than those obtained with non-diagonal distortions, and we came to strongly think that the best candidate to be the “natural” distortion is the one associated with the Kurdjumov-Sachs orientation relationship [20]. In-situ experiments on nano-objects could help to determine the “natural” distortions associated with mechanical twinning and phase transitions.

### As twinning is not shearing, how to replace the Schmid factor?

The calculations showed that there is a volume variation during extension twinning (Fig. 3) and, since the distance OV also changes (Fig. 6b), the twinning plane can't be let fully invariant. It is true that when the transformation finishes, i) the volume comes back to its initial value, ii) the twinning plane is fully restored, and iii) the distortion matrix becomes a simple shear matrix; however, the details of the mechanism between the initial and final state can't and shouldn't be ignored; twinning is definitively not shearing. What is the consequence? The Schmid factor used to calculate the resolved shear stress on the twinning plane is not adapted anymore to predict the twin formation. Is it possible to substitute the Schmidt law by another one? Could it explain some of the abnormalities observed in the formation of the extension twins (see section 1)?

It is reasonable to think that the volume change observed during the lattice distortion introduces an energy barrier that should be overcome to form the twins. This idea was also suggested for the fcc-bcc martensite transformations [20]. If this assumption is correct, it would mean that instead of using the matrix of complete transformation, i.e. the simple shear matrix (24), one should use the intermediate matrix corresponding to the maximum volume change, i.e. the matrix given by

equation (22) with  $\kappa = \kappa_i$ . Since this matrix is not a simple shear matrix a criterion substituting the Schmidt law should be found. We propose to come back to the general formula giving the interaction work  $W$  of a unit volume of a material that deforms, by mechanical twinning or phase transformation, inside an external stress field  $\Gamma$ . The scalar  $W$  is given by the Frobenius inner product

$$W = \Gamma_{ij} \cdot \mathcal{E}_{ij} \quad (29)$$

which is simply the integral form of the infinitesimal work  $dW = \Gamma_{ij} \cdot d\mathcal{E}_{ij}$  for uncorrelated fields  $\Gamma$  and  $\mathcal{E}$ . The work is performed by the external stress during the transformation. A high value of interaction work means a high probability of transformation, and negative value should correspond to an impossibility of transformation. The interaction energy is the opposite of  $W$ ; it should be added to the usual form of energy that is calculated to predict a phase transformation. Maximizing the interaction work is equivalent to minimizing the interaction energy. As proved in Appendix A, the interaction work is proportional to the Schmid factor in the case of a simple shear. Let us illustrate this situation for extension twinning. The numerical value of the final distortion matrix is given in the basis  $\mathbf{B}_{ortho}$  by equation (24):

$$\mathbf{D}_f^{p \rightarrow t} = \mathbf{D}_{ortho}^{p \rightarrow t}(1/3) \approx \begin{pmatrix} 1 & 0 & 0 \\ 0 & 0.9412 & 0.0624 \\ 0 & -0.0555 & 1.0588 \end{pmatrix} \quad (30)$$

Now, let us consider a Mg parent crystal that is rotated by an angle  $\theta$  around the direction  $\mathbf{n}$  normal to  $(0\bar{1}12)$  plane, and tilted by an angle  $\phi$  around the  $\mathbf{x}$ -axis. The matrix of rotation of angle  $\phi$  around the  $\mathbf{x}$ -axis, and the matrix of rotation of angle  $\theta$  around the  $\mathbf{n}$ -axis are noted  $\mathbf{R}_x(\phi)$  and  $\mathbf{R}_n(\theta)$ , respectively. As showed in equation [A4] of Appendix A, the distortion matrix of the rotated-tilted parent crystal, still expressed in the basis  $\mathbf{B}_{ortho}$ , becomes

$$\mathbf{D}_f^{p \rightarrow t}(\phi, \theta) = \mathbf{R}_x(\phi) \mathbf{R}_n(\theta) \cdot \mathbf{D}_f^{p \rightarrow t} \cdot (\mathbf{R}_x(\phi) \mathbf{R}_n(\theta))^{-1} \quad (31)$$

The twinning deformation is given by the matrix  $\mathcal{E}_f^{p \rightarrow t}(\phi, \theta) = \mathbf{D}_f^{p \rightarrow t}(\phi, \theta) - \mathbf{I}$ . According to equation (29), its interaction work with a stress field  $\Gamma$  is

$$W_f(\phi, \theta) = \Gamma_{ij} \cdot (\mathcal{E}_f^{p \rightarrow t})_{ij}(\phi, \theta) \quad (32)$$

The graph of interaction work  $W_f(\phi, \theta)$  in the case of a uniaxial stress along the  $\mathbf{z}$ -axis is given in Fig. 9a. As expected, it is similar to the graph obtained for a simple shear (Fig. A3); the only difference is that the interaction work is maximum for a shear plane tilted at  $\phi = 45^\circ$  in the case of Fig. A3, whereas it is maximum for a crystal tilted at  $\phi = 2^\circ$  for extension twinning. This is due to the fact that the  $(0\bar{1}12)$  shear plane is already tilted  $43^\circ$  far from the basal plane in a crystal positioned horizontally, which means that a tilt of  $\phi_s = 2^\circ$  is sufficient to place the shear plane at  $45^\circ$  from the  $\mathbf{z}$ -axis. Actually, all the matrices of simple shear exhibit the same graph of interaction work and differ only by translating the origin of the  $(\phi, \theta)$  axes. According to the matrix  $\mathbf{D}_f^{p \rightarrow t}$ , the extension twins can form only for positive interaction work, i.e. for tilt angles  $\phi_s - \frac{\pi}{4} < \phi < \phi_s + \frac{\pi}{4}$ , i.e. in the range of tilt angle  $\phi \in [-43^\circ, 47^\circ]$ . What happens if the intermediate distortion matrix is used in place of the simple shear matrix? The numerical values of the intermediate distortion matrix corresponding to maximal volume change is given in the basis  $\mathbf{B}_{ortho}$  by equation (22) with  $\kappa = \kappa_i$ :

$$\mathbf{D}_i^{p \rightarrow t} = \mathbf{D}_{ortho}^{p \rightarrow t}(\kappa_i) \approx \begin{pmatrix} 1 & 0 & 0 \\ 0 & 0.9852 & 0.0308 \\ 0 & -0.0290 & 1.0449 \end{pmatrix} \quad (33)$$

This matrix is used to calculate the intermediate distortion matrix  $\mathbf{D}_i^{p \rightarrow t}(\phi, \theta)$  in a parent crystal tilted around the  $\mathbf{x}$ -axis by an angle  $\phi$ , and rotated around the  $\mathbf{n}$ -axis by an angle  $\theta$ , as in equation (31). The intermediate deformation matrix is  $\mathcal{E}_i^{p \rightarrow t}(\phi, \theta) = \mathbf{D}_i^{p \rightarrow t}(\phi, \theta) - \mathbf{I}$ . This matrix, instead of  $\mathcal{E}_f^{p \rightarrow t}(\phi, \theta)$ , is now used in equation (32) to calculate the interaction work  $W_i(\phi, \theta)$  at the intermediate state. The graph of  $W_i(\phi, \theta)$  in the case of a uniaxial stress along the  $\mathbf{z}$ -axis is given in Fig. 9b. It is clear that the region of positive work  $W_i$  is extended in comparison with  $W_f$ . For  $\theta = 0$ , which means that the shear direction is not rotated in the twinning plane and is kept at its maximum value (only the parent crystal is tilted), the interaction work  $W_i$  is positive in the range of tilt angles  $\phi \in [-59^\circ, 59^\circ]$ , whereas  $W_f$  is positive only in the range  $[-43^\circ, 47^\circ]$ . In other words, the use of the intermediate distortion matrix and a criterion based on interaction work allows the predictions of formation of extension twins for some domains of orientations where the classical Schmid factor is negative. The full domains can be clearly defined by calculating the values  $(\phi, \theta)$  where  $W_i \geq 0$  and  $W_f < 0$ . The graph is shown in Fig. 9c. It gives the orientations where our model predicts extension twinning whereas classical theory does not. Since the experiments are often realized by tilting the parent crystal around the  $\mathbf{z}$ -axis instead of the  $\mathbf{n}$ -axis (because  $\mathbf{n}$  depends on which of the six twinning variants is formed), we have plotted in Fig. 10 the same graphs as those of Fig. 9, but now substituting the rotation  $\mathbf{R}_z(\theta)$  by the rotation  $\mathbf{R}_n(\theta)$ , as illustrated by the comparison of Fig. 10d with Fig. 9d. Of course, the results are the same as Fig. 9 along the line  $\theta = 0$ . The range  $\phi \in [-59^\circ, 59^\circ]$  predicted by our model is exactly the range of formation of extension twins deduced by Čapek *et al.* [13] by extrapolating a series of neutron diffraction measurements on polycrystalline Mg deformed by tensile tests at different strains (see Fig. 6a of ref. [13]). The agreement with some experimental data is promising. However, besides this encouraging sign, we should admit that there are many experiments reported in literature that we can't yet explain. We calculated the interaction work for some stress fields implying compression components, but the graphs giving the values  $(\phi, \theta)$  where  $W_i \geq 0$  and  $W_f < 0$  were reduced to zero, which means that our model can't do better than the classical theory for compressive stresses. It doesn't mean that our approach is wrong because it is possible that for such configurations, the "anomalous" formation of deformation twins is due to a local stress field that is different from the applied stress field, as suggested by Jonas *et al.* [11]. Only further precise experiments on Mg single crystals could help to discriminate the classical model based on the Schmid law from our model based on the interaction work at maximum volume change. Fig. 10c will be useful for to interpret the results of these experimental tests.

## 8. Conclusion

Our previous crystallographic works on martensitic transformations in steels and other alloys [20][21] showed that shear or invariant plane strain matrices are not appropriate to evaluate the atomic displacements and lattice distortion of displacive transformations. We proposed to substitute them by angular-distortive matrices whose continuous analytical expressions can be calculated with a simple hard-sphere model. Here, we applied a similar approach to the problem of  $\{10\bar{1}2\}$  extension twins in Mg alloys. The case of the  $\{10\bar{1}1\}$  compression twins and the so-called  $\{10\bar{1}1\}$ - $\{10\bar{1}2\}$  double twins will be the subject of a second paper. The step flow of our approach is opposite

to the classical theory. Instead of determining the simple shears that could restore the lattice, and then guessing the trajectories of the atoms that are not at the lattice nodes (shuffles), we first calculated the atom trajectories assuming that they are hard-sphere of constant size, and then we calculated the analytical expression of the lattice distortion. The advantage is that it is sure that the atoms do not interpenetrate each other during the distortion, i.e. the energetical barriers remain reasonable during the transformation path. During the distortion, the unit volume increases up to 3% and the length of the “diagonal” direction in the twinning plane (direction OV) increases up to 1.4%, before both coming back to their initial values when the transformation is complete. Then, and only then, the distortion matrix becomes a simple shear matrix. The  $\{10\bar{1}2\}$  twinning plane is not fully invariant during the distortion; it is just globally invariant, i.e. untilted and fully restored when the distortion is finished. These results confirm that extension twinning is not a shear mechanism.

The calculations also showed that the tetragonal distortion, deduced by Liu et al.[17] from their observations of  $(90^\circ, \mathbf{a})$  twinning domains in a submicron-sized Mg pillar, is a component by polar decomposition of the distortion matrix associated with the usual  $(86^\circ, \mathbf{a})$  domains of  $\{10\bar{1}2\}$  extension twins in bulk Mg. The atom trajectories are very similar in the two cases and differ only by a rotation of  $3.5^\circ$ . This means that the Liu et al.’s observations are in agreement with the displacive character of mechanical twinning, and can’t be considered as a sign for a fully reconstructive mechanism. An analogy with ferroelectrics made us think that the tetragonal distortion associated with the  $(90^\circ, \mathbf{a})$  domains could be a “spontaneous” distortion, and that the usual distortion associated with the  $(86^\circ, \mathbf{a})$  domains could be a “constrained” one. The  $3.5^\circ$  compensating angle can then be viewed as an obliquity angle.

As twinning is not shearing, a criterion was introduced to replace the classical Schmid law. It is based on the interaction work between an external stress field and the deformation field generated by the twinning distortion. The criterion allowed us to predict the formation of extension twins for parent crystal orientations with negative Schmid factors. More precisely, the model predicts the formation extension twins during uniaxial tensile tests with parent crystals tilted in the range  $[-59^\circ, 59^\circ]$  whereas the usual model predicts extension twins only in the range  $[-43^\circ, 47^\circ]$ . The fact that a critical tilt angle of  $59^\circ$  was already experimentally reported is very encouraging.

## Acknowledgments

I would like to show my gratitude to Prof. Roland Logé, director of LMTM, and to PX group for the laboratory subsidy and for our scientific and technical exchanges.

# Appendix A

The aim of this appendix is to show that the Schmidt factor for a simple shear deformation is a special case of a more general criterion based on the interaction work between an external stress field and a internal strain field.

The shear matrix of amplitude  $s$  along the [100] direction on the (001) shear plane is

$$\mathbf{S} = \begin{pmatrix} 1 & 0 & s \\ 0 & 1 & 0 \\ 0 & 0 & 1 \end{pmatrix} \quad [\text{A1}]$$

This situation is illustrated in Fig. A1a. Now, let us consider that the same shear occurs in a crystal that is rotated around  $\mathbf{z}$  by an angle  $\theta$  and tilted around  $\mathbf{x}$  by an angle  $\phi$ , as shown in Fig. A1b. The two rotation matrices are noted  $\mathbf{R}_x(\phi)$  and  $\mathbf{R}_z(\theta)$  respectively, and illustrated in Fig. A2. They are

$$\mathbf{R}_x(\phi) = \begin{pmatrix} 1 & 0 & 0 \\ 0 & \cos\phi & -\sin\phi \\ 0 & \sin\phi & \cos\phi \end{pmatrix} \text{ and } \mathbf{R}_z(\theta) = \begin{pmatrix} \cos\theta & -\sin\theta & 0 \\ \sin\theta & \cos\theta & 0 \\ 0 & 0 & 1 \end{pmatrix} \quad [\text{A2}]$$

One way to deduce the new shear matrix is to write it from the new shear plane normal  $\mathbf{n}$  and shear vector  $\mathbf{s}$  given by

$$\mathbf{n}(\phi) = \mathbf{R}_x(\phi) \cdot [001] = \begin{bmatrix} 0 \\ -\sin\phi \\ \cos\phi \end{bmatrix} \quad [\text{A3}]$$

$$\mathbf{s}(\theta) = \mathbf{R}_x(\phi) \cdot \mathbf{R}_z(\theta) \cdot [010] = \begin{bmatrix} -\sin\theta \\ \cos\phi \cdot \cos\theta \\ \sin\phi \cdot \cos\theta \end{bmatrix}$$

The other way is to write directly the shear (active) matrix  $\mathbf{S}$  in the rotated crystal by:

$$\mathbf{S}(\phi, \theta) = \mathbf{R}_x(\phi) \cdot \mathbf{R}_z(\theta) \cdot \mathbf{S} \cdot (\mathbf{R}_x(\phi) \cdot \mathbf{R}_z(\theta))^{-1} \quad [\text{A4}]$$

The two methods gives the same result for the shear matrix [A1] :

$$\mathbf{S}(\phi, \theta) = \begin{pmatrix} 1 & \sin\theta \cdot \sin\phi \cdot s & -\cos\phi \cdot \sin\theta \cdot s \\ 0 & 1 - \cos\theta \cdot \cos\phi \cdot \sin\phi \cdot s & \cos\theta \cdot \cos^2\phi \cdot s \\ 0 & -\cos\theta \cdot \sin^2\phi \cdot s & 1 + \cos\theta \cdot \cos\phi \cdot \sin\phi \cdot s \end{pmatrix} \quad [\text{A5}]$$

The shear displacements are given by the matrix  $\mathbf{S}(\phi, \theta) - \mathbf{I}$ . When they occur inside a stress field  $\boldsymbol{\Gamma}$ , a work is performed; it is the product of force along the displacements. When the strain field and the stress field are not correlated, this work is

$$W(\phi, \theta) = \boldsymbol{\Gamma}_{ij} \cdot \boldsymbol{\varepsilon}_{ij}(\phi, \theta) \quad [\text{A6}]$$

with the Einstein convention on the repetition of the indices  $(i,j)$ .

Let us consider the simple case of a uniaxial stress  $\sigma_z$  applied along the  $\mathbf{z}$  direction, i.e.

$$\Gamma = \begin{pmatrix} 0 & 0 & 0 \\ 0 & 0 & 0 \\ 0 & 0 & \sigma_z \end{pmatrix} \quad [A7]$$

The interaction work becomes

$$W(\phi, \theta) = \sigma_z \cdot (\cos\theta \cdot \cos\phi \cdot \sin\phi) \cdot s = \sigma_z m s = \tau s \quad [A8]$$

where  $\tau$  is the shear stress and  $m$  is Schmid factor, usually given by form  $m = \cos\phi \cdot \cos\lambda$  with  $\lambda$  the angle between the direction  $\mathbf{z}$  and the shear vector  $\mathbf{s}$ . From the expression [A3] it is easy to see that  $\cos\lambda = \sin\phi \cdot \cos\theta$ , and that, indeed,  $m = \cos\phi \cdot \sin\phi \cdot \cos\theta$ . The advantage of the expression  $m = \cos\phi \cdot \sin\phi \cdot \cos\theta$  in comparison to the classical form  $m = \cos\phi \cdot \cos\lambda$  is that the two angles  $\theta$  and  $\phi$  are not correlated, whereas the angle  $\lambda$  is a function of the angle  $\phi$ . For instance, it could be thought that it is possible to maximize  $m$  by choosing  $\phi = 0$  and  $\lambda = 0$ , but this is not true due to the correlation of the two angles. With the expression  $m = \cos\theta \cdot \cos\phi \cdot \sin\phi$ , it is easy to see that  $m$  is maximized for  $\phi = \frac{\pi}{4}$  and  $\theta = 0$ .

The interaction work [A8] is simply the work performed by the shear stress along the shear displacement. The interaction energy is the opposite value of the interaction work. It is an energy by unit of volume and is expressed, as  $\sigma_z$ , in MPa (for the units remember that Pa = J/m<sup>3</sup>). Therefore, the Schmid factor, used to introduce a critical resolved shear stress, is equivalent to a critical interaction energy. As for the Schmid factor, one can plot the interaction work depending on the orientation of the crystal. The graph of  $W(\phi, \theta)$  is given in Fig. A3. It can be checked that the interaction energy is maximum at  $(\phi, \theta) = \left(\frac{\pi}{4}, 0\right)$  and  $(\phi, \theta) = \left(-\frac{\pi}{4}, \pi\right)$ . It is important to note that this is just a special case of the equation [A6]. The big advantage of equation [A6] lays in its generality; it doesn't depend on the type of distortion and can be applied to non-shear distortions. For example, the well-known Patel-Cohen equation [28] that gives the interaction energy for an invariant plain strain (simple shear + deformation perpendicularly to the habit plane) is also a special case of equation [A6].

# References

- [1] M.A. Jaswon, D.B. Dove, The Crystallography of Deformation Twinning, *Acta Cryst.* 13 (1960) 232-240.
- [2] B.A. Bilby, A.G. Crocker, The Theory of the Crystallography of Deformation Twinning, *Proc. R. Soc. Lond. A.* 288 (1965) 240-255.
- [3] M. Bevis, A.G. Crocker, Twinning Shears in Lattices, *Proc. Roy. Soc. Lond. A.* 304 (1968) 123-134.
- [4] J.W. Christian, S. Mahajan, Deformation Twinning, *Prog. Mater. Sci.* 39 (1995) 1-157.
- [5] A.G. Crocker, M. Bevis, The Science Technology and Application of Titanium, ed. R. Jaffee and N. Promisel, Pergamon Press, Oxford (1970), 453-458.
- [6] M. Niewczas, Lattice correspondence during twinning in hexagonal close-packed crystals, *Acta Mater.* 58 (2010) 5848-5857.
- [7] B.C. Wonsiewicz, W.A. Backofen, Plasticity of magnesium crystals. *Trans. Metall. Soc. AIME* 239 (1967) 1422-1431.
- [8] M. D. Nave, M.R. Barnett, Microstructures and textures of pure magnesium deformed in plane-strain compression, *Scripta Mater.* 51 (2004) 881-885.
- [9] M.R. Barnett, Z. Keshavarz, A.G. Beer, X. Ma, Non-Schmid behavior during secondary twinning in a polycrystalline magnesium alloy, *Acta Mater.* 56 (2008) 5-15.
- [10] J.R. Luo, A. Godfrey, W. Liu, Q. Liu, Twinning behavior of a strongly basal textured AZ31 Mg alloy during warm rolling, *Acta Mater.* 60 (2012) 1986-1998.
- [11] J.J. Jonas, S. Mu, T. Al-Samman, G. Gottstein, L. Jiang, E. Martin, The role of strain accommodation during the variant selection of primary twins in magnesium, *Acta Mater.* 59 (2011) 2046-2056.
- [12] B. Wang, L. Deng, N. Guo, Z. Xu, Q. Li, EBSD analysis of {10-12} twinning activity in Mg-3Al-1Zn alloy during compression, *Mater. Charact.* 98 (2014) 180-185.
- [13] J. Čapek, K. Máthis, B. Clausen, J. Stráská, P. Beran, P. Lukáš, Study of the loading mode dependence of the twinning in the random textured cast magnesium by acoustic emission and neutron diffraction methods, *Mater. Sci. Engng A* 602 (2014) 25-32.
- [14] K.D. Molodov, T. Al-Samman, D.A. Molodov, G. Gottstein, On the role of anomalous twinning in the plasticity of magnesium, *Acta Mater.* 103 (2016) 711-723.
- [15] S. Yu, C. Liu, Y. Gao, S. Jiang, Z. Chen, A rotation-shear model on the atomic motion during {10-12} twinning in magnesium alloys, *Mater. Lett.* 165 (2016) 185-188.
- [16] R.C. Pond, J.P. Hirth, A. Serra, D.J. Bacon, Atomic displacements accompanying deformation twinning: shears and shuffles, *Mater. Res. Lett.* (2016) DOI: 10.1080/21663831.2016.1165298.

[17] B.-Y. Liu, J. Wang, B. Li, L. Lu, X.-Y. Zhang, Z.-W Shan, J. Li, C.-L. J, J. Sun, E. Ma, Twinning-like lattice reorientation without a crystallographic plane, *Nat. Com.* 5:3297 (2014) doi: 10.1038/ncomms4297.

[18] B.-Y. Liu, J. Wang, B. Li, L. Lu, X.-Y. Zhang, Z.-W Shan, Terrace-like morphology of the boundary created through basal-prismatic transformation in magnesium, *Scripta Mater.* 100 (2015) 86-89.

[19] A. Ostapovets, J. Buršík, R. Gröger, Deformation due to migration of faceted  $\{10\bar{1}2\}$  twin boundaries in magnesium and cobalt, *Phil. Mag.* 95 (2015) 1-12.

[20] C. Cayron, Continuous atomic displacements and lattice distortion during fcc–bcc martensitic transformation, *Acta Mater.* 96 (2015) 189-202.

[21] C. Cayron, Angular distortive matrices of phase transitions in the fcc-bcc-hcp system, *Acta Mater.* 111 (2016) 417-441.

[22] H.K.D.H Bhadeshia (2001), Worked examples on the geometry of crystals, free book at [www.msm.cam.ac.uk/phase-trans/2001/geometry2/Geometry.pdf](http://www.msm.cam.ac.uk/phase-trans/2001/geometry2/Geometry.pdf)

[23] P.R. Potnis, N.-T. Tsou, J.E. Huber, A Review of Domain Modelling and Domain Imaging Techniques in Ferroelectric Crystals, *Materials* 4 (2011) 417-447.

[24] M. Otoničar, S.D. Škapin, B. Jančar, R. Ubic, D. Suvorov, Analysis of the Phase Transition and the Domain Structure in  $K_{0.5}Bi_{0.5}TiO_3$  Perovskite Ceramics by In Situ XRD and TEM, *JACS* 93 (2010) 4168-4173.

[25] J. Fousek, V. Janovec, The Orientation of Domain Walls in Twinned Ferroelectric Crystals, *JAP* 40 (1969) 135-142.

[26] J. Sapriel, Domain-wall orientations in ferroelastics, *Phys.Rev. B* 12 (1975) 5128-5140.

[27] C. Cayron, Groupoid of orientational variants, *Acta Cryst. A* 62 (2006) 21-40.

[28] J.R. Patel, M. Cohen, Criterion for the action of applied stress in the martensitic transformation, *Acta Metall.* 1 (1953) 531-538.

# Figures

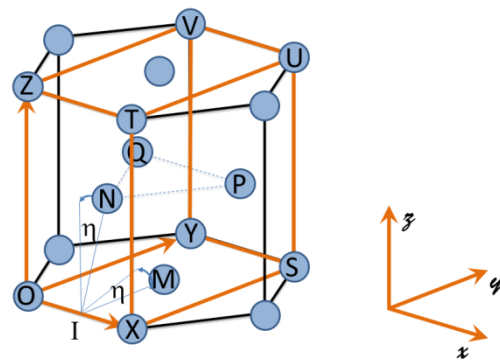
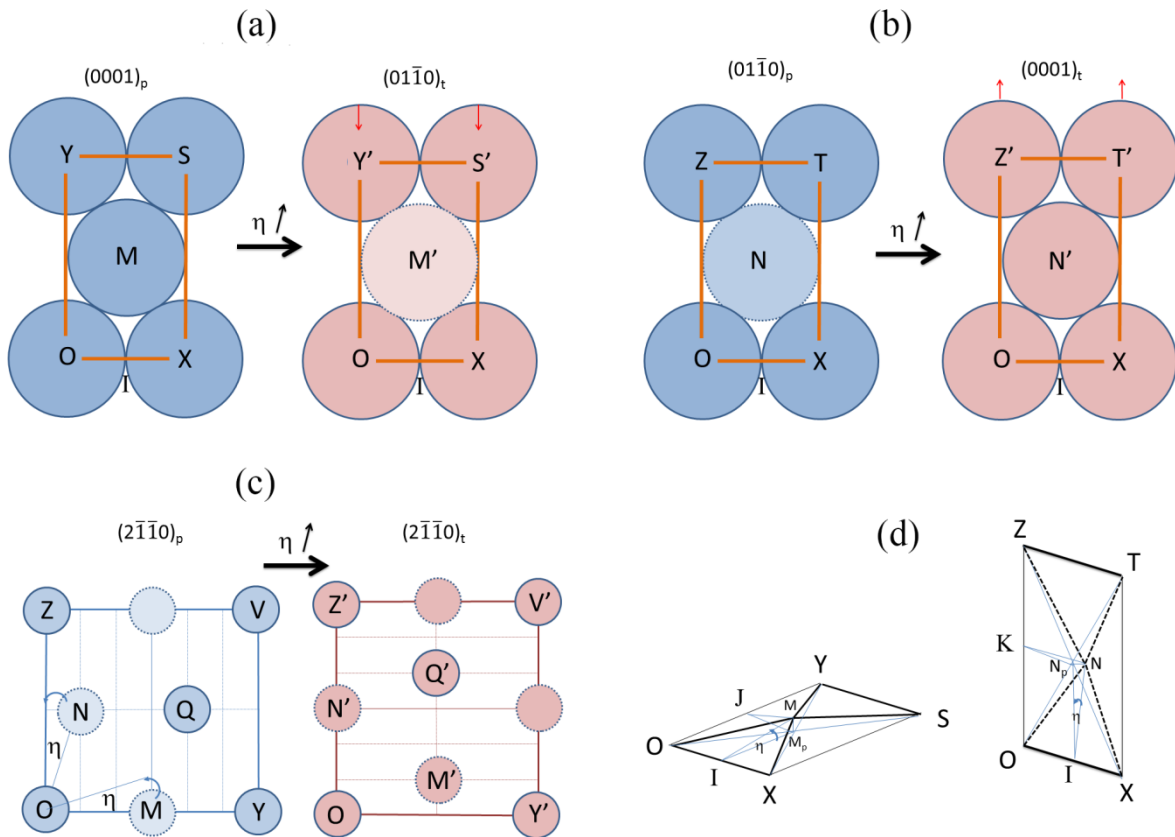


Fig. 1. Hexagonal lattice of the parent crystal with its associated orthonormal basis  $(x, y, z)$ ,  $x = a_p$ ,  $y = 2a_p + b_p$ ,  $z = c_p$ . Some positions of the Mg atoms are labeled in order to describe the atomic displacement during the extension twinning process. The angle  $\eta$  is used as the unique parameter of the lattice distortion.



*Fig. 2. Schematic representation of the atomic displacements and lattice distortion during extension twinning viewed on different planes of the parent crystal: a) on  $OXY = (0001)_p$ , b) on  $OXZ = (01\bar{1}0)_p$ , c) on  $OYZ = (2\bar{1}\bar{1}0)_p$  planes. The parent crystal is in blue and its resulting extension twin is in salmon. All the atomic displacements are functions of a unique parameter, i.e. the angle  $\eta$  of rotation of the M atom around the  $OX$  axis. The vector  $OX = \mathbf{a}$  remains invariant. The distance  $OY$  decreases to become  $OY'$ , and the  $(0001)_p$  plane is transformed into the  $(01\bar{1}0)_t$  plane. The distance  $OZ$ , initially  $OZ = c$ , increases to eventually become  $OZ' = a$  when the distortion is complete, and the  $(01\bar{1}0)_p$  plane is transformed into the  $(0001)_t$  plane. (d) Schemes explaining the change of the distances  $OY$  and  $OZ$ : as the atom M moves far from plane  $(OXY)$ , the distance  $OY$  decreases, and as the atom N moves toward the plane  $(OXZ)$ , the distance  $OZ$  increases. During the process, the hard-sphere packing assumption imposes that  $MO = MX = MY = MS = NO = NX = NT = NT = OX =$  (atom diameter).*

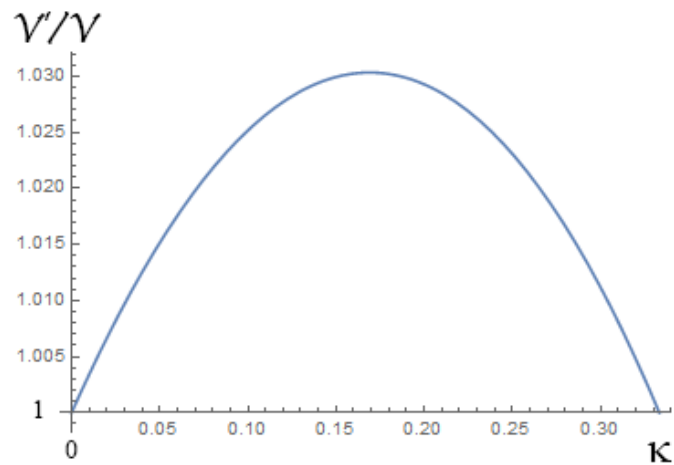


Fig. 3. Change of volume ratio  $V'/V$  during extension twinning, function of the parameter  $\kappa = \sin(\eta)$ , varying from  $\kappa_s = 0$  (start) to  $\kappa_f = 1/3$  (finish).

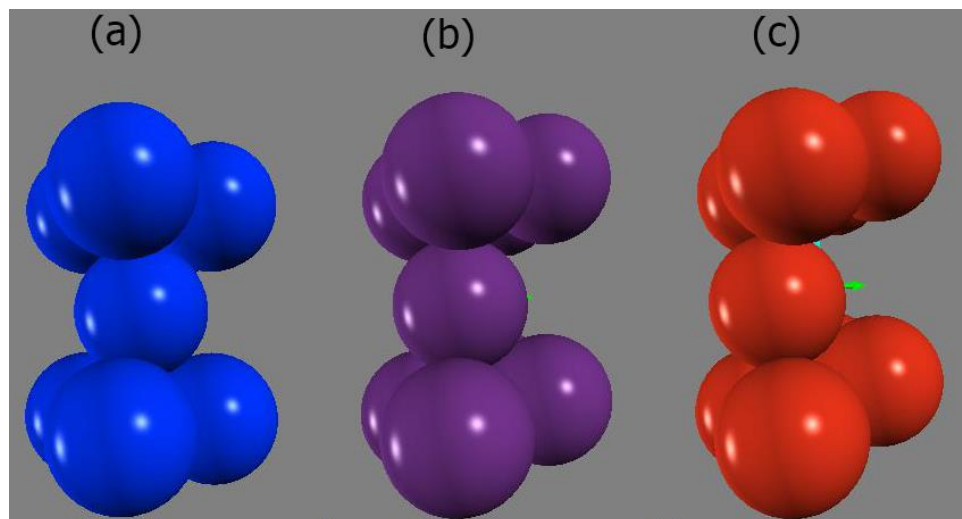


Fig. 4. 3D view of the stretch distortion with a hexagonal Bravais unit cell. (a) Initial hcp cell ( $\eta = 0$ ), with the  $(0001)_p$  plane horizontal and  $(01\bar{1}0)_p$  plane vertical, (b) intermediate state ( $\eta = 9^\circ$ ), and (c) final state ( $\eta \approx 20^\circ$ ). The final state is a restored hcp structure, but with the basal and prismatic planes interchanged in comparison with (a).

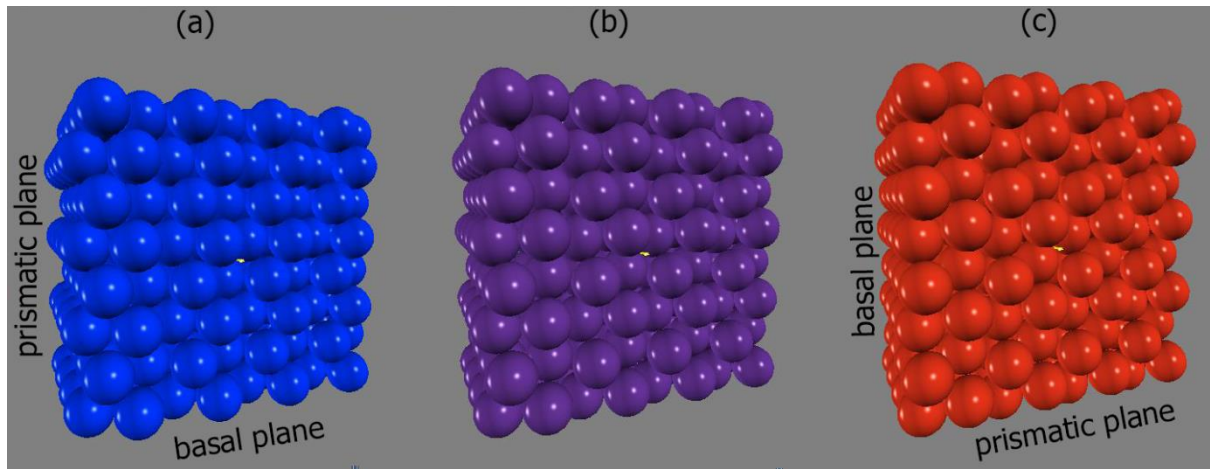


Fig. 5. 3D view of the stretch distortion of a crystal made with  $4 \times 4 \times 4$  XYZ cells. (a) Initial hcp cell ( $\eta = 0$ ), (b) intermediate state ( $\eta = 9^\circ$ ), and (c) final state ( $\eta \approx 20^\circ$ ). The basal and prismatic planes interchanged during the distortion

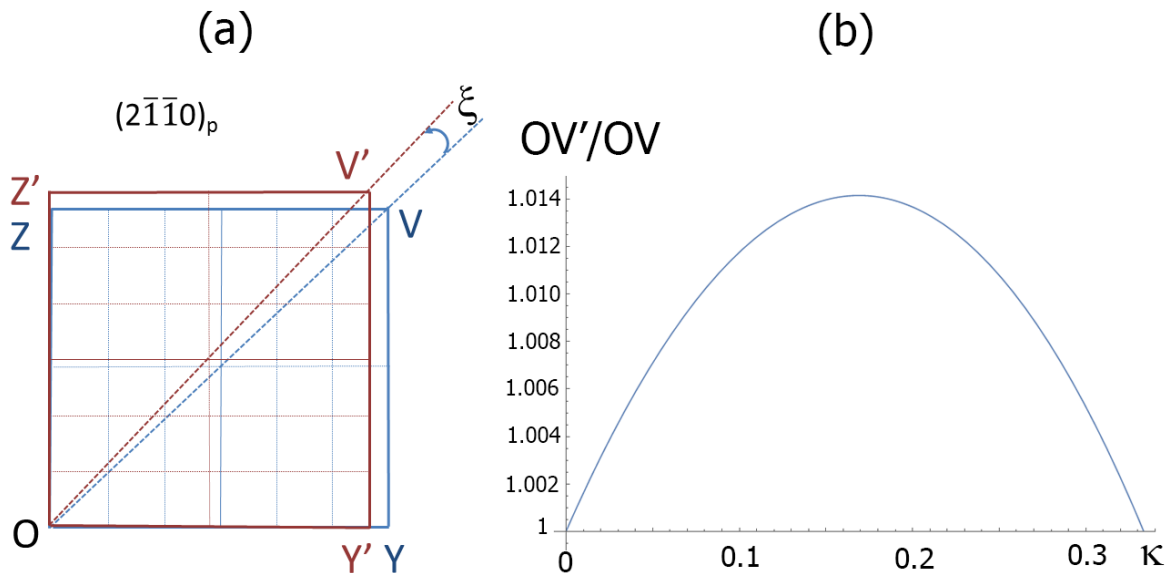


Fig. 6. Change of the direction  $OV$  during twinning distortion. (a) Schematic view on the plane  $OYZ = (2\bar{1}\bar{1}0)_p$  of the tilt  $\xi$  of  $OV$  around the  $a$ -axis. (b) Evolution of the ratio of distances  $OV'/OV$  proving that even if the tilt  $\xi$  is corrected, the  $(0\bar{1}12)$  plane cannot be maintained fully invariant.

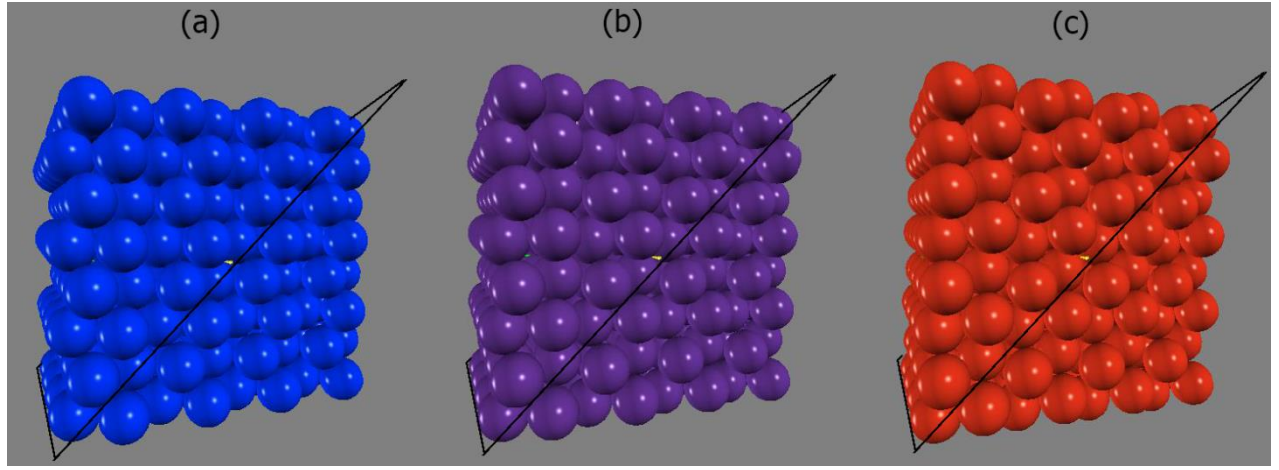


Fig. 7. 3D view of the distortion associated with  $\{10\bar{1}2\}$  extension twinning with a crystal made with  $4 \times 4 \times 4$  XYZ cells. (a) Initial hcp cell ( $\eta = 0$ ), (b) intermediate state ( $\eta = 9^\circ$ ), and (c) final state ( $\eta \approx 20^\circ$ ). The hcp structure is restored but the basal and prismatic planes interchanged while the  $(0\bar{1}12)$  plane is maintained untilted. The  $(0\bar{1}12)$  plane is marked by the black section.

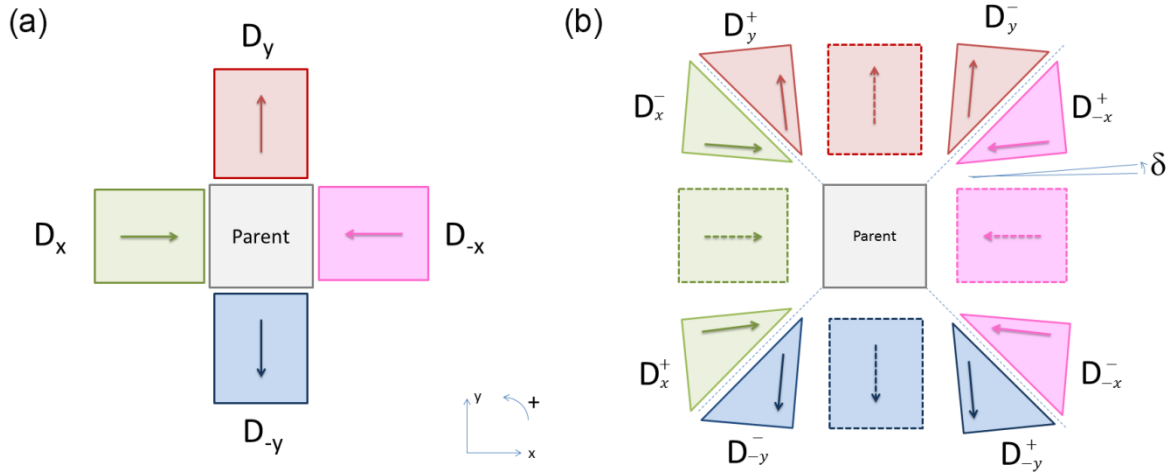
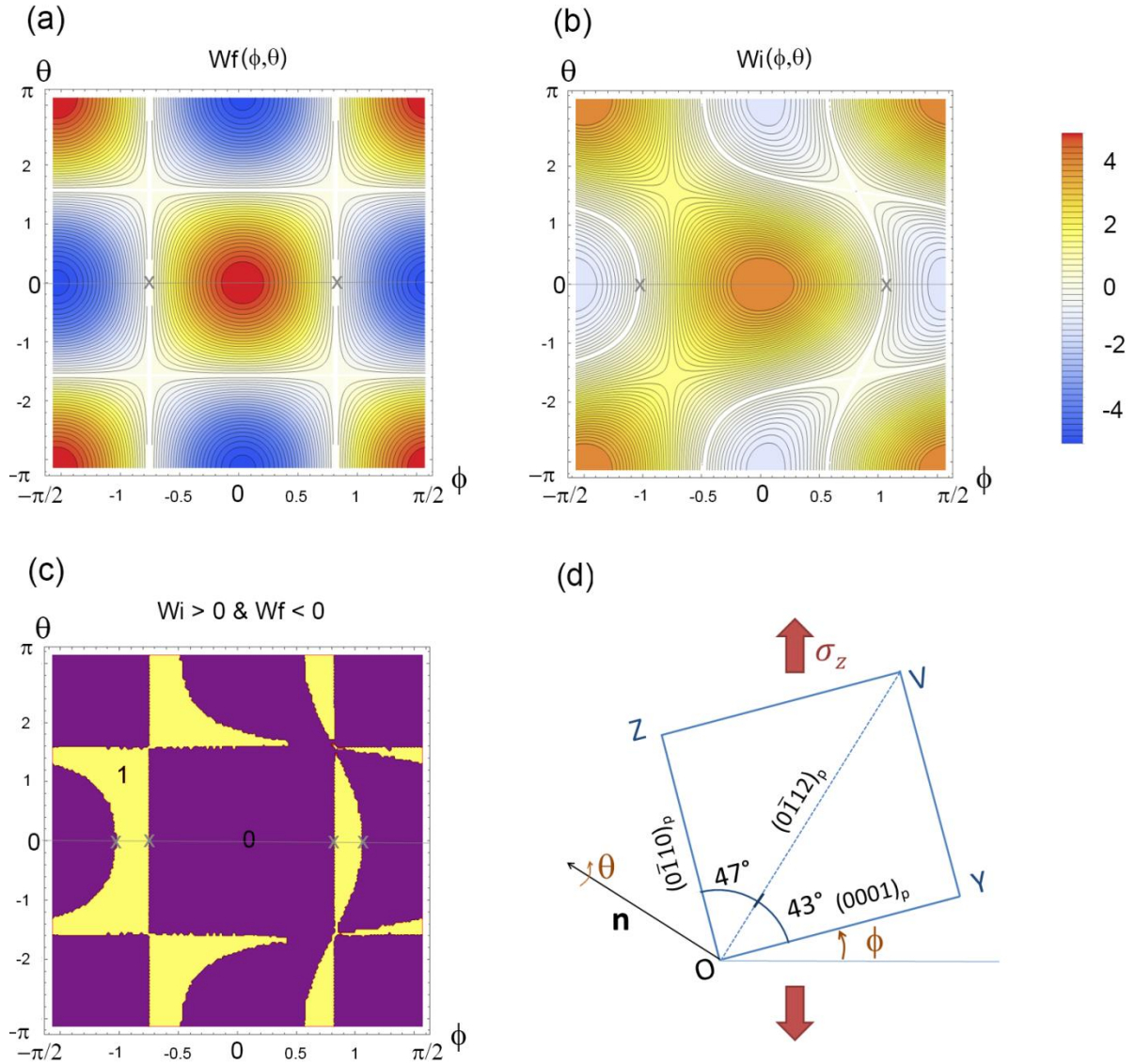
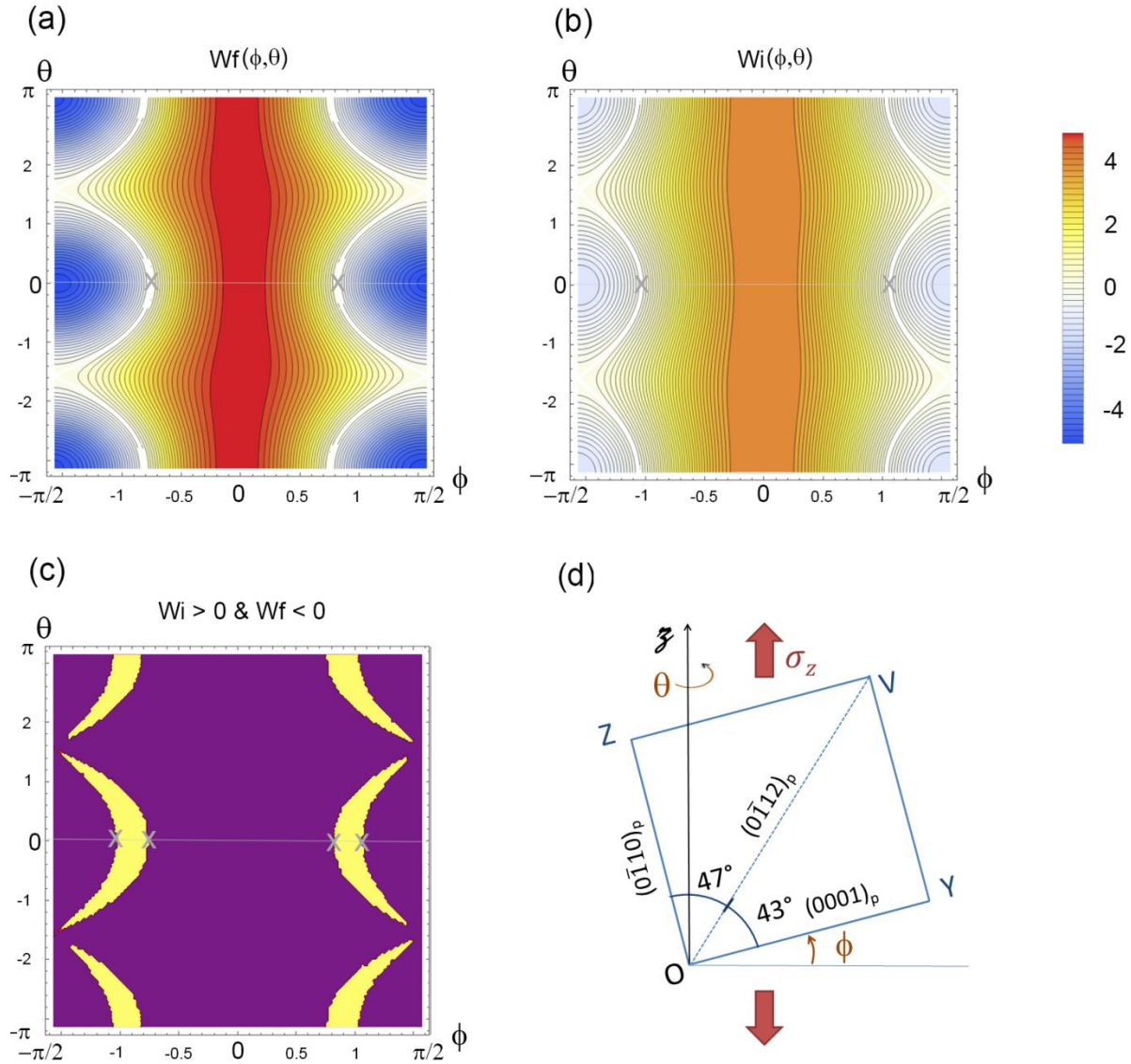


Fig. 8. 2D representation of the orientational domains in a ferroelectric crystal created by a cubic  $\rightarrow$  tetragonal phase transition. (a) Domains of "spontaneous" distortion with the polarization vectors (arrows) along the high-symmetry  $x$  and  $y$ -axes. (b) Domains experimentally observed, with domain walls on the  $(1,1)$  and  $(1,-1)$  planes. A small rotation of the spontaneous domains by an angle  $\delta$ , called obliquity, is required to respect the compatibility conditions at the interfaces. There are 4 variants in case (a) and 8 in case (b).



*Fig. 9. Interaction work (in MPa) during extension twinning in a tensile stress field oriented along the  $z$ -axis of a parent crystal tilted by an angle  $\phi$  around the  $a$ -axis and rotated by an angle  $\theta$  around the  $n$ -axis (normal to the twinning plane). a) Interaction work  $W_f$  calculated with the complete distortion (shear) matrix.  $W_f$  is proportional to the usual Schmid factor. b) Interaction work  $W_i$  calculated with the intermediate distortion matrix corresponding to the maximum volume change. c) Graph showing in yellow the orientations  $(\phi, \theta)$  where the condition  $W_i > 0 \text{ and } W_f < 0$  is true, i.e. where the criterion based on  $W_i$  could explain the twin formation despite negative Schmid factors ("anomalous" twins). The axes in the graphs are in radians. d) Schematic view of the orientation of the parent crystal. The segments delineating the domains  $W_f > 0$  and  $W_i > 0$  for  $\theta = 0$  are marked by the grey crosses in a) and b), respectively.*



*Fig. 10. Interaction work (in MPa) during extension twinning in a tensile stress field oriented along the  $\mathbf{z}$ -axis of a parent crystal tilted by an angle  $\phi$  around the  $\mathbf{a}$ -axis and rotated by an angle  $\theta$  around the  $\mathbf{z}$ -axis (and not  $\mathbf{n}$ -axis as in the previous figure). a) Interaction work with the complete shear matrix. b) Interaction work  $W_i$  with the intermediate distortion matrix corresponding to the maximum volume change. c) Graph showing in yellow the orientations  $(\phi, \theta)$  where the condition  $W_i > 0$  &  $W_f < 0$  is true is true, i.e. where the criterion based on  $W_i$  could explain the twin formation despite negative Schmid factors (“anomalous” twins). The axes in the graphs are in radians. d) Schematic view of the orientation of the parent crystal. The segments delineating the domains  $W_f > 0$  and  $W_f > 0$  for  $\theta = 0$  are marked by the grey crosses in a) and b), respectively.*

## Appendix Figures

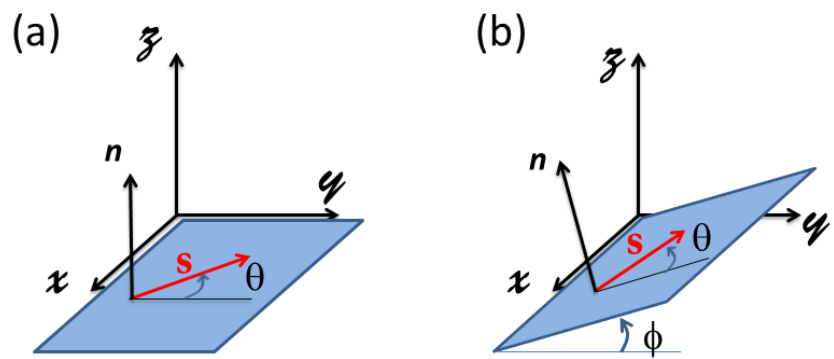


Fig. A1. Schematic view of a simple shear with the shear vector  $s$  that is rotated by an angle  $\theta$  in the shear plane of normal  $n$ . a) The shear plane is horizontal, and b) the shear plane is tilted by an angle  $\phi$  around the  $x$ -axis.

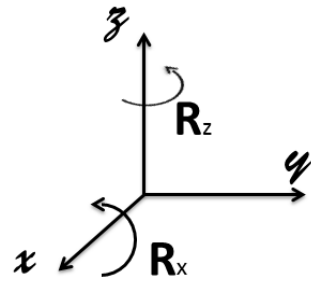
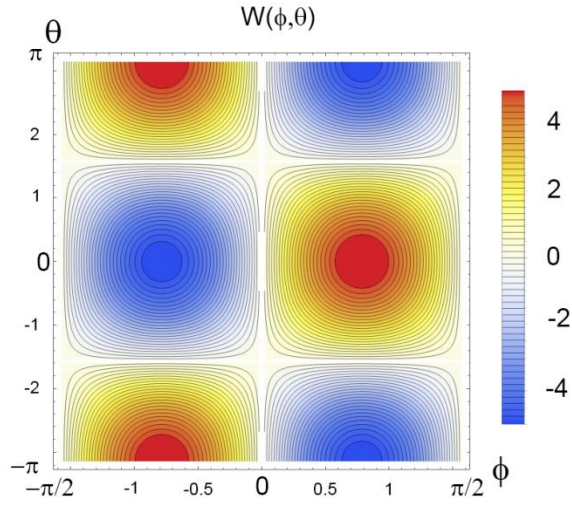


Fig. A2. Graphic representation of the two rotations  $R_x$  and  $R_z$ .



*Fig. A3.* Interaction work (in MPa) performed by a simple shear distortion that occurs in a tensile stress field oriented along the  $z$ -axis with a parent crystal that is tilted by an angle  $\phi$  around the  $x$ -axis and rotated by an angle  $\theta$  around the  $n$ -axis, as illustrated in Fig. A1b. The graph is calculated from equation [A8] with  $\sigma_z = 100$  MPa and  $s = 0.1$ . The maximum and minimum values are obtained in the red and blue area, respectively; they are  $W_{max} = 5$  MPa and  $W_{min} = -5$  MPa.